



ELSEVIER

Surface Science 470 (2000) 1–14



www.elsevier.nl/locate/susc

Solution of the $p(2 \times 2)$ NiO(1 1 1) surface structure using direct methods

N. Erdman^{a,*}, O. Warschkow^b, D.E. Ellis^b, L.D. Marks^a

^a *Institute for Environmental Catalysis, Department of Materials Science and Engineering, Northwestern University, 2225 N. Campus Drive, Evanston, IL 60208, USA*

^b *Institute for Environmental Catalysis, Department of Physics and Astronomy, Northwestern University, Evanston, IL 60208, USA*

Received 25 July 2000; accepted for publication 22 September 2000

Abstract

A solution for the $p(2 \times 2)$ NiO(1 1 1) surface reconstruction was obtained using direct methods applied to X-ray diffraction data. The solution was refined with 296 data points and 21 parameters using χ^2 minimization ($\chi^2 = 1.82$, $R = 0.17$). The surface atoms showed very small relaxation from the bulk interatomic distances (Ni–Ni distances are 2.9 ± 0.1 Å; Ni–O -2.0 ± 0.1 Å). The solution can be characterized by alternating close-packed layers of oxygen and nickel atoms: the top surface layer is nickel terminated with 3/4 of the nickel atoms missing, the next oxygen layer is completely full, and the third, nickel layer, has 1/4 of the nickel atoms missing. The structure is consistent with theoretical predictions of octopolar termination of the surface and exhibits the features observed by previous STM studies. In addition, local density functional calculations have been carried out in this work in order to gain insights into the surface charge distribution and electronic structure of the proposed reconstruction. Calculated partial atomic charges and magnetic moments as well as densities of state are reported. The cation deficient nature of the surface requires the presence of electron holes for charge compensation, which we find mainly located on second layer oxygen atoms. The structure differs from that recently reported for the same surface, and we are not able to reproduce the reported good fit to the (same) experimental data. © 2000 Elsevier Science B.V. All rights reserved.

Keywords: Computer simulations; Nickel oxides; Surface relaxation and reconstruction; X-ray scattering, diffraction, and reflection; Faceting

1. Introduction

Transition metal oxides have been studied extensively over the last few decades, due to their electro-optical and catalytic properties [1,2]. The overall properties of these oxides and the hetero-

structures that can be built on them depend upon the surface structure, composition and morphology. However, the available information on the surface structures of transition metal oxides is very scarce and often contradictory.

The NiO(1 1 1) surface is known to exhibit important physical and chemical properties – NiO is antiferromagnetic at low temperature [3] and a catalytic compound [4,5]. The alternating layers of Ni^{2+} and O^{2-} ions produce a non-vanishing dipole moment perpendicular to the surface, resulting in

* Corresponding author. Tel.: +1-847-491-3267; fax: +1-847-491-7820.

E-mail address: n-erdman@nwu.edu (N. Erdman).

an unstable bulk terminated NiO(111) polar surface with a nominally infinite surface energy [6]. Theoretical calculations for ionic crystals with NaCl-type structures have predicted two similar solutions to this problem: either the clean unreconstructed (111) surface will facet into neutral {100} type planes upon annealing, or a reconstruction of the surface will occur (i.e. faceting on an atomic scale) [7]. Some of these results [8,9] indicate a possible ‘octopolar’ termination of the NaCl(111) surface, which should be stable at zero temperature. The basic structural unit of such a surface will be a simple cubic (NaCl)₄ octopolar unit, instead of the conventional face-centered cubic (f.c.c) lattice with a dipolar Na⁺–Cl[–] basis. Using atomistic modeling techniques, Oliver et al. [10] investigated the dependence of NiO surface energy with respect to surface oxidation (i.e. concentration of Ni vacancy/electron hole aggregates). They found an oxidized nickel-terminated NiO(111) surface to be energetically more stable than an unoxidized surface.

Recent investigations indeed indicate that a stable NiO(111) surface can be obtained experimentally. Schofield et al. [11] observed a stable ($\sqrt{3} \times \sqrt{3}$)R30° reconstruction on an NiO(111) surface, after annealing the surface in air at 800°C for 1.5 h. The surface reconstruction was characterized using transmission high-energy electron diffraction (THEED), RHEED and XPS and the surface structure determined using direct methods was found to contain triangular oxygen features. Ventrice et al. [12] reported a stable p(2 × 2) reconstruction for NiO films grown on Au(111) at 550 K using low energy electron diffraction and STM. The STM images showed a stable reconstruction characterized by relatively flat (corrugation <0.2 Å) terraces with a step height of ~2.4 Å and several missing-atom point defects. The images showed features that were interpreted as micropyramidal structures (three-atom clusters with the atom of opposite charge located above each cluster) on the surface; however, the authors were not able to conclude whether the micropyramids were oxygen- or nickel-terminated. Barbier et al. [13,14] investigated the p(2 × 2) NiO(111) reconstruction on both a single crystal surface and a 5 monolayer thick NiO(111) thin film grown on

Au(111) using GIXS. For a single crystal p(2 × 2) reconstructed surface the authors proposed a model with a Ni-terminated octopolar reconstruction and double steps. The thin film exhibited different structural features and the proposed model had an equal combination of Ni-terminated and O-terminated octopolar terraces on the surface separated by single steps, leading to coexistence of two different surface phases. Unfortunately, the thin film reconstruction model contradicts the previous STM results [12] that showed a single structure. Furthermore, as will be discussed in more detail below, we are unable to reproduce their reported fit to the experimental data.

In a diffraction experiment, the amplitudes of the reflections are recorded, but the phase information is lost, thus preventing a direct Fourier inversion of the data. The measured amplitudes allow calculation of the Patterson function (e.g. see Ref. [15]), which provides interatomic vector information. Unfortunately a Patterson function analysis is often problematic due to ambiguities in picking out individual interatomic vectors and the presence of artifacts. The latter is a severe problem for surfaces where only a limited number of reflections are measured. In this paper we report the use of direct methods to determine the atomic structure of the p(2 × 2) surface using the thin-film GIXS diffraction data [14] and propose an alternative reconstruction that is cation deficient.

First principles density functional (DF) calculations were carried out on the proposed surface structure in order to understand the local electronic properties and these were compared to similar calculations on atomistically relaxed octopolar reconstructions with Ni- and O-termination.

2. Methodology

2.1. Direct methods

Diffraction techniques provide a powerful tool for the refinement of atomic positions; however, they require an initial model that is relatively close to the ‘true’ structure for the refinement to work. Information about the phases of the structure

factors that is lost in a diffraction experiment is necessary to restore the charge density or scattering potential (X-ray or electron diffraction, respectively). This problem has been solved for bulk X-ray diffraction using an approach called direct methods. In the last few years, the direct methods approach has been successfully applied to two-dimensional (2D) X-ray diffraction data to solve surface structures [16,17], and more recently for 3D data [18]. This approach solves the phase problem by exploiting probability relationships between the amplitudes and the phases of the diffracted beams. Effectively, a set of plausible models for the structure is generated, starting only from the intensity data.

The method used for the $p(2 \times 2)$ NiO(111) structure involved a minimum relative entropy algorithm combined with a genetic algorithm for global optimization (for more details, see Refs. [19,20]). The algorithm searches for the set of phases with the lowest figures of merit (FOM). The solutions with the lowest FOMs are used to create electron density maps that obey the imposed symmetry. If the experimental errors are very small or non-existent, these maps can approach an accurate charge density restoration. However, sometimes only a part of the structure can be identified in the initial analysis, due to measurement errors or insufficient information on the symmetry of the structure.

For this analysis, the X-ray diffraction data collected for the NiO(111) film grown on an Au(111) surface were used. Details of the sample preparation and the collection of the GIXS data have been reported elsewhere [14]. A total of 25 independent intensities in the 2D $p6mm$ (Patterson) plane group and in 3D 296 independent reflections in $p3m1$ symmetry were considered for the calculations. Since $p6mm$ Patterson symmetry may correspond to $p3$, $p3m1$, $p31m$ or $p6mm$ plane group symmetries, all of those were considered in the calculations.

Full 3D calculations were also performed, followed by refinement by replacing peaks in the maps by atoms and allowing the positions of these atoms to vary. In the final step, the atomic positions were refined using the least-squares method with the *SHELX-97* program [21]. The agreement

between the measured and the calculated intensities was calculated using two different parameters. The *R*-factor is defined as:

$$R = \frac{\sum ||F_0| - |F_c||}{\sum |F_0|}$$

where F_0 is the measured structure factor, F_c is the calculated structure factor. In addition, the χ^2 value was calculated:

$$\text{Goodness of Fit} = \chi^2 = \left\{ \frac{\sum [w(F_0^2 - F_c^2)^2]}{(n - p)} \right\}$$

where n is the number of reflections and p is the total number of parameters refined. The effect of lattice vibrations on the diffracted beam amplitudes, and therefore on the final solution, was included in the final steps of the refinement fixing the Debye–Waller factors for the subsurface atoms to those of the NiO crystal lattice. We used isotropic Debye–Waller factors for NiO which have previously been determined via a polynomial expansion with temperature [22] in the form:

$$B(T) = a_0 + a_1T + a_2T^2 + a_3T^3 + a_4T^4$$

where T is in Kelvin, B is given in \AA^2 , and a_i are polynomial fitting parameters. The temperature factors used in the refinement were calculated for 300 K.

A few points need to be made about the experimental data, which in raw form was the same as that used previously [13,14]. We received three X-ray diffraction data sets from Dr. Barbier for the (2×2) reconstruction of NiO(111) surface. The first set was data for a single crystal surface reconstructed after annealing in air. According to Dr. Barbier, only the in-plane measurements were reliable, a total of 16 reflections. The second data set (a single crystal after UHV annealing) consisted of 9 in-plane and 39 out-of-plane reflections (the latter were not averaged and were for only two different rods). For both data sets the number of reflections was too small to attempt a structure determination. The third data set (a 5 ML NiO(111) thin film grown on Au(111)) was the most complete one with 321 measurements, and the results of the direct methods calculations for this data set are presented in this paper [23]. The 2D symmetry of NiO(111) is $p3m1$, so the

Patterson symmetry (i.e. the symmetry of the intensities) should be $p6mm$ in the plane, $P3(\text{bar})m1$ in three dimensions. The raw data contained large deviations from this required symmetry, which we averaged out by applying the required symmetry operations. (Even if the surface is of lower symmetry, unless there is strong preference for a particular domain due to a miscut surface it is impossible not to have the full symmetry in the intensities.) It should be noted that it is not permissible to use $p3m1$ for intensity data as was done previously [13,14].

2.2. Electronic structure calculations

DF calculations were performed in the local spin density approximation (LSDA, $X_\alpha = 0.7$ exchange-correlation) in the framework of the discrete variational (DV) method [24–26]. Calculations were performed using a linear scaling divide-and-conquer (DAC) ansatz [27–30], which describes every symmetry-unique atom in the system at hand by a local cluster of atoms (a fragment) embedded into the effective Kohn–Sham potential of all other atoms. In this way, the system is effectively described in a patchwork approach by many overlapping embedded clusters, each designed to accurately describe a local region of the system. Fragments interact with each other through the effective potential. Charge transfer between fragments is facilitated by imposition of a common chemical potential. Near-minimal numerical atomic orbital basis sets have been used in all calculations. The oxide basis set consists of

O-1s, 2s and 2p atomic orbitals calculated for a free anion, which was embedded into a potential well to ensure bound solutions. The nickel cation basis set includes atomic orbitals 1s, 2s, . . . , 3d, 4s and 4p. The frozen core approximation was applied to core orbitals up to and including O-1s and Ni-3s. To facilitate evaluation of the Coulomb potential, electron densities were least-squares fitted to an auxiliary fit basis set of spherically symmetric density fit functions which are derived from the orbital basis set. DAC fragments were generated by adding to the atom described by the fragment all atoms within a radius of $R_F = 7.5$ a.u. as “buffer atoms” (see Ref. [29]). With this cut-off, clusters containing 27 atoms describe atoms in bulk NiO. Fragments for atoms near the surface contain fewer atoms. All reported partial charges were calculated using Mulliken partitioning of electron densities. All density of states (DOS) diagrams were generated by convoluting the discrete spectrum of partitioned fragment orbitals with Lorentzian distributions of width 0.1 eV.

Single point LSDA calculations on the NiO(111) $p(2 \times 2)$ reconstruction were performed using a three-dimensionally periodic slab model of the surface. In this model, a slab consists of 17 layers (9Ni, 8O), which – as will become evident later – ensures that the central layers of the slab are sufficiently removed from the surface to be bulk-like. The atomic positions for the outermost five layers are set to the experimental structure (see Table 1). All deeper layers are fixed to bulk structure. The slab model thus has a total thickness of about 19 Å; along the (111) direction

Table 1

Atom positions for the solution in terms of $p(2 \times 2)$ unit cell in $p3m1$ plane group with $a = b = 5.8970$ Å, $c = 72.226$ Å, $\alpha = \beta = 90^\circ$, $\gamma = 120^\circ$

Layer	Atom	x	y	z (Å)
1 (surface)	Ni1	$2/3$	$1/3$	0
2 (surface)	O1	$1/3$	$2/3$	–1.2109(4)
	O2	0.3160(120)	0.1580(60)	–0.6313(4)
3 (surface)	Ni2	0.5008(5)	0.4992(5)	–2.2951(5)
4 (bulk)	O3	$2/3$	$1/3$	–3.4457(9)
	O4	0.1640(30)	0.3290(60)	–3.4992(8)
5 (bulk)	Ni3	$1/3$	$2/3$	–4.7388(4)
	Ni4	0.3261(7)	0.1631(4)	–4.6831(4)
6 (bulk)	O5	0	0	–5.5429(5)
	O6	0.4895(18)	0.5105(18)	–5.4295(3)

successive slabs are separated by approximately 21 Å of vacuum. The slab unit cell contains 16 symmetry unique atoms, each of which is described by its own DAC fragment. An antiferromagnetic alignment of magnetic moments on Ni sites between successive (111) layers has been imposed.

For reference, we have calculated charge and electronic structure of bulk-NiO with antiferromagnetic (AF2) alignment of magnetic spins. Partial atomic charges are calculated to be $\pm 1.73 e$ with a magnetic moment of $1.71 \mu_B$ on Ni. The calculated DOS is displayed in Fig. 1, which shows a broad Ni-band around the Fermi level (E_F) with a d-d gap of $\sim 0.5 eV$ as well as an O-2p band at lower energy in good agreement with previously reported LSDA calculations on this material (e.g. Refs. [31,35]). In the local density approximation NiO is described as a Mott-type semi-conductor, with a narrow d-d type band gap. We note that there is considerable controversy in the literature over the nature of this gap and the apparent inability of LSDA to describe the late transition metal oxides as charge-transfer semiconductors has been well documented [31–35]. However, we believe that these intricacies bear little effect on the present purpose of establishing the approximate distribution of surface charge near NiO(111).

2.3. Atomistic simulations

Atomistic simulations were performed on two octopolar reconstructions of NiO(111). As in the DFT model, surfaces in the atomistic simulations were represented using a surface slabs of 17 atomic layers in the [111] direction. The surface atomic structure is described using Ni^{2+} and O^{2-} point atom species interacting through a Born model potential including electrostatic, short-range Buckingham, and Shell-model polarization effects. The parameterization of the pair potential model used in this work is that given by Yan et al. [36], derived for and employed in the calculation of NiO surface energies. In this work, atomistic relaxation was applied only to the Ni- and O-terminated octopolar reconstructions [13,14] because they are both stoichiometric and can thus be described with a fair degree of confidence by an atomistic pair potential model. In contrast, the ap-

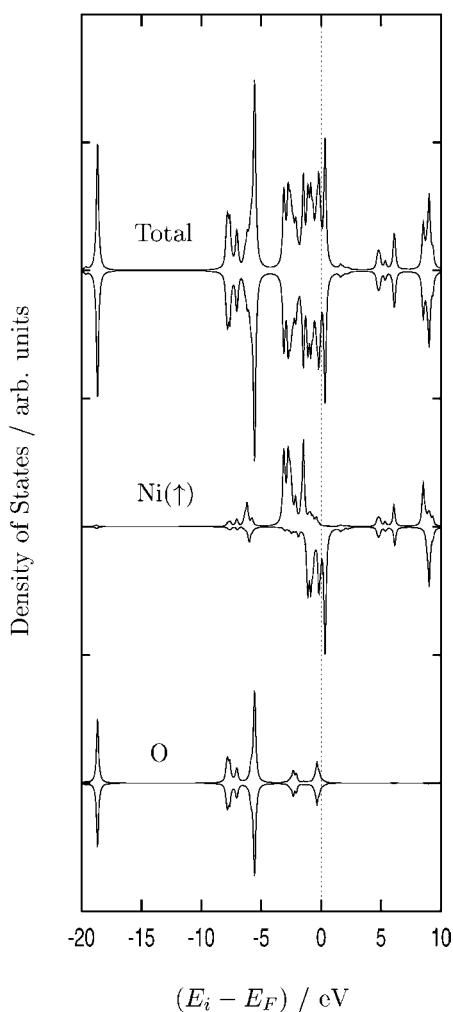


Fig. 1. Spin polarized, total and local DOS calculated for bulk NiO (antiferromagnetic). Energies are relative to the Fermi-level. The local DOS of the spin-down Ni site – Ni(\downarrow), not shown in this figure, is the negative of that for the spin-up site Ni(\uparrow).

plication of atomistic relaxation to the non-stoichiometric reconstruction proposed in this work (see below) is considerably more problematic – and was avoided for this reason – because there is little empirical guidance as to how pair interactions change upon introduction of charge compensating electron holes. All atomistic calculations were performed using the GULP package [37,38], kindly provided by Dr. J.D. Gale.

3. Results

The charge density maps calculated using 2D diffraction data showed plausible solutions only for the $p3$ and $p3m1$ plane groups (see Fig. 2). Full 3D calculations were performed for both these groups and are shown in Fig. 3. The data set (296 independent reflections) was refined using 21 parameters to describe the model. The corresponding R -factor is 0.17, and the χ^2 value is 1.82. The top surface layer is nickel-terminated, with 3/4 of the nickel atoms missing, the next oxygen layer is completely full, and the third (nickel) layer has 1/4 of its nickel atoms missing. Atom positions for both Ni and O are shown in Table 1, and the final model for the $p(2 \times 2)$ surface structure in Fig. 4. The surface atoms showed only very small relaxation from bulk interatomic distances. The surface layer Ni–Ni distance is $2.9 \pm 0.1 \text{ \AA}$, and the Ni–O distance $2.0 \pm 0.1 \text{ \AA}$. The bond angles are almost

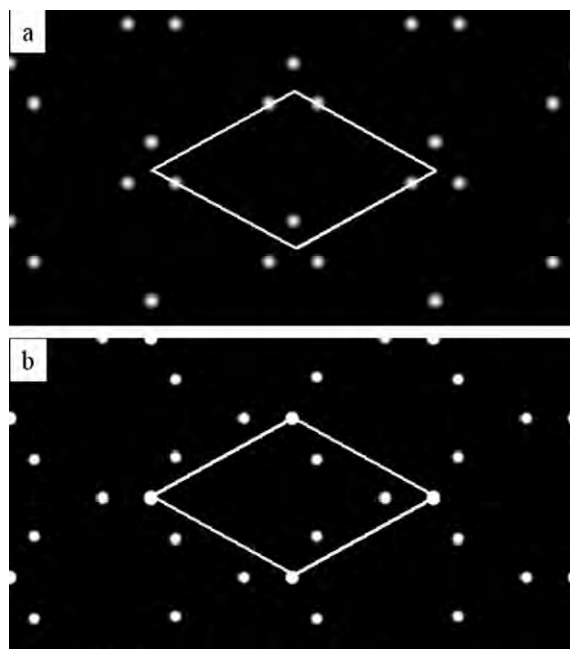


Fig. 2. Charge density maps calculated using the 2D code corresponding to (a) $p3$ and (b) $p3m1$ symmetries. The primitive unit cell is indicated with solid lines ($a = b = 5.8970 \text{ \AA}$, $\gamma = 120^\circ$). White regions correspond to high charge density, the probable locations of atoms.

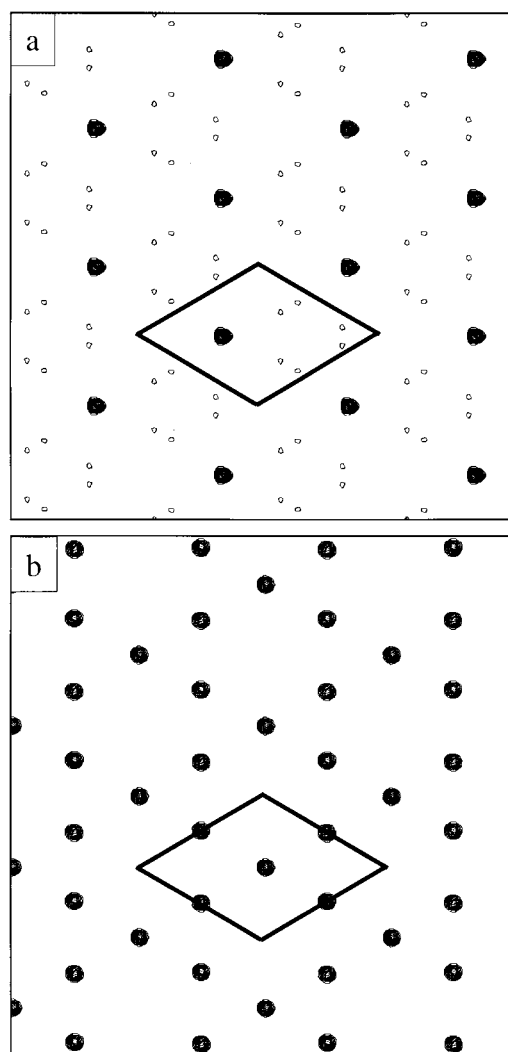


Fig. 3. Contour maps obtained from 3D code for $P3m1$ symmetry. Shown are two out of 39 'slices' along the z -axis, separated by 2.257 \AA ; (a) shows the top (1st) Ni layer with 3/4 of the Ni atoms missing, and (b) shows the underlying (3rd) Ni layer with 1/4 of the Ni atoms missing. The primitive unit cell is indicated with solid lines ($a = b = 5.8970 \text{ \AA}$, $\gamma = 120^\circ$). The dense contour regions (essentially black) are the sites of the Ni atoms.

exactly the same as in the bulk structure. Since this reconstruction is cation-deficient (i.e. Ni_{1-x}O), we will refer to it in the following as *non-stoichiometric*, and *oxidized*, when contrasting it to the alternative *stoichiometric* octopolar reconstruction proposed by Barbier et al. [13,14].

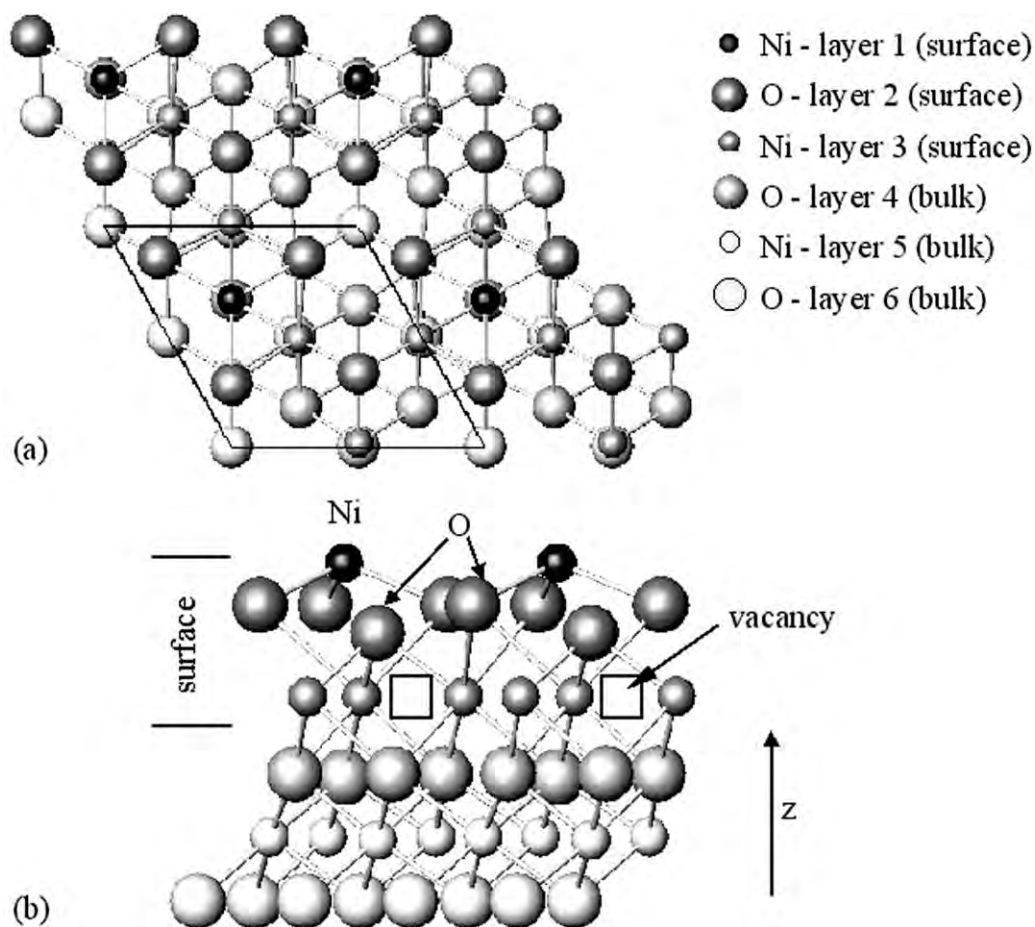


Fig. 4. (a) Top view of the oxidized $p(2 \times 2)$ NiO(111) surface structure obtained by direct methods analysis. (b) Side view of the structure. The solution is characterized by $1/4$ of the Ni atoms removed from the second layer and put on the surface in a 2×2 configuration (Schottky defect formation).

Comparison between the experimental and calculated intensities for various diffraction rods is shown in Fig. 5. Note that for some of the rods (e.g. -45 L), the intensities observed close to the origin were relatively small; application of an appropriate scaling factor for the intensities in this case has some justification and would have improved the fit (we did not attempt to rescale the rods). We attempted to reproduce the reported fit to the (same) experimental data using octopoles [13,14] that has been previously published using both the standard Shelx code as well as the Rods code. While it was possible to obtain a reasonable value for χ^2 , the R -factor was exceedingly high

(about 0.7) even when domains of Ni and O terminated octopoles were considered. With large experimental errors it is possible to overfit weak intensities and poorly fit the strong ones obtaining a misleadingly small value of χ^2 but a large value for the R -factor. All attempts to refine using as a starting point the octopole atomic location were completely unstable and led to major changes in the atomic positions. We are forced to conclude that the good fit previously reported is in error, probably due to incorrect treatment of the symmetry requirements.

If one considers our reconstruction as being made up solely of Ni^{2+} and O^{2-} building blocks,

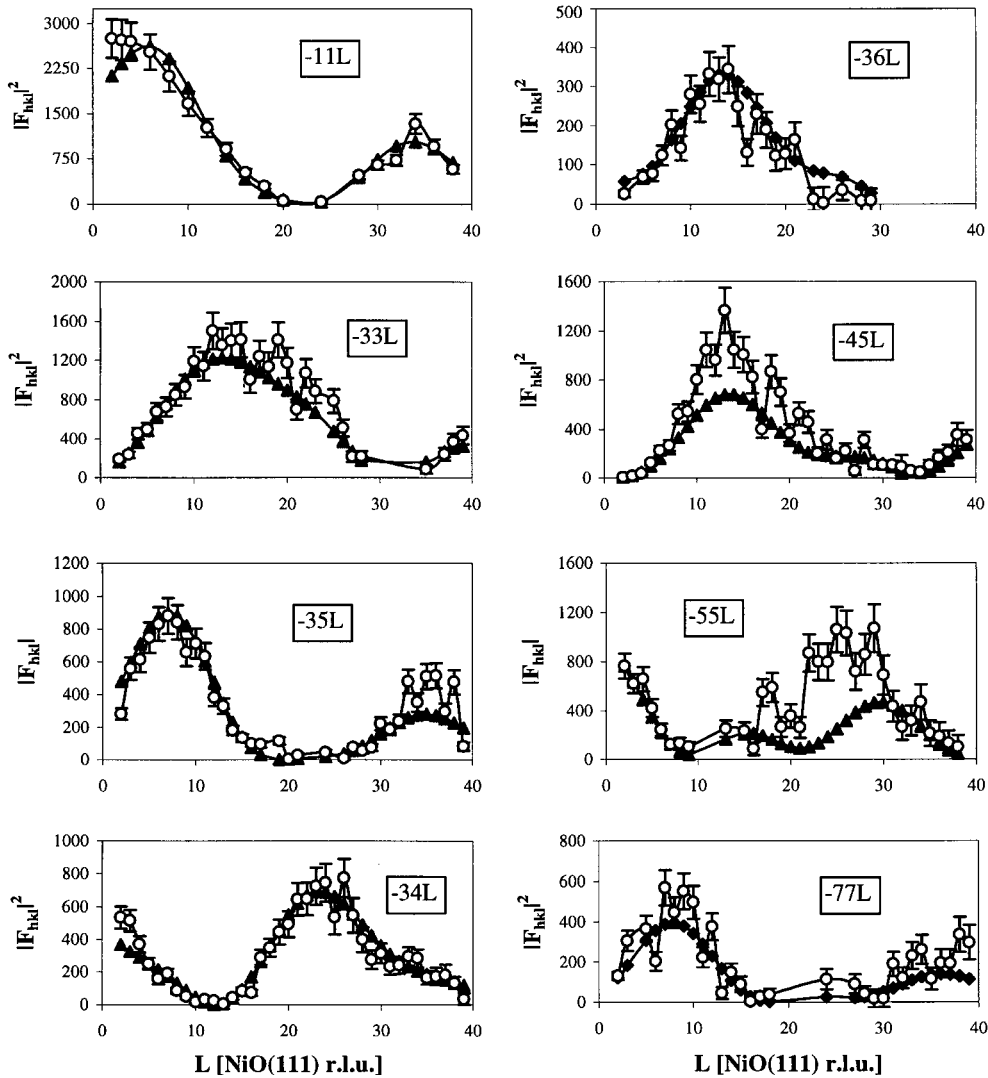


Fig. 5. Comparison of measured (○) and calculated (▲) intensities for various diffraction rods for the $p(2 \times 2)$ reconstruction. The h and k indexes are expressed in the (2×2) r.l.u.

simple charge accounting reveals that four electrons per $p(2 \times 2)$ surface unit would have to be removed from the system in order that a zero surface charge is attained. Formally this can be accomplished by raising the oxidation state of four atoms per surface unit, e.g. Ni^{2+} to Ni^{3+} or O^{2-} to O^{1-} , as has been done in recent empirical potential models of NiO(111) surface reconstruction (e.g. Ref. [10]). However, in a more adequate description, the distribution of these surface holes around

surface atoms is more “fluid”, with non-integer changes in partial atomic charges. Insights into the peculiarities of this distribution can be gained from electronic structure calculations.

The calculated partial atomic charges and magnetic moments for the surface slab model are listed in Table 2. In Fig. 6, the local densities of states (LDOS) for the top six layers have been profiled which should be contrasted with those in bulk NiO (Fig. 1). First of all, one can see that

Table 2
Calculated partial charges and magnetic moments for the oxidized NiO(111) p(2 × 2) reconstruction

Layer	Atom	Charge/e (moment/ μ_B)
1 (surface)	Ni1 (1×)	+1.37 (+1.24)
2	O1 (1×)	-1.19 (-0.83)
	O2 (3×)	-0.83 (-0.60)
3	Ni2 (3×)	1.59 (-1.59)
4	O3 (1×)	-1.67 (+0.12)
	O4 (3×)	-1.56 (+0.10)
5	Ni3 (1×)	+1.80 (+1.55)
	Ni4 (3×)	+1.83 (+1.76)
6	O5 (1×)	-1.75 (-0.01)
	O6 (3×)	-1.72 (-0.04)
7	Ni5 (1×)	+1.75 (-1.72)
	Ni6 (3×)	+1.73 (-1.72)
8	O7 (1×)	-1.73 (+0.01)
	O8 (3×)	-1.73 (+0.01)
9	Ni7 (1×)	+1.74 (+1.71)
	Ni8 (3×)	+1.73 (+1.71)
Bulk	Ni	+1.73 (± 1.71)
Bulk	O	-1.73 (± 0.00)

charges and magnetic moments in the deep layers are almost identical to those calculated for the bulk. The same is found for the LDOS of the deep lying layers of the slab model – not displayed in Fig. 6 – which are virtually indistinguishable from those in the bulk. This is to a lesser extent already evident in the displayed LDOS for sites O5, O6 and Ni4, which show only little deviation from bulk (Fig. 6). This gives confidence in the model since it apparently describes adequately the complete transition of the electronic structure from surface to bulk.

Looking now at the surface effects, we find those largely localized to the top five atomic layers, with the two oxygen atom types (O1 and O2) in the second layer exhibiting large reductions in ionicity and surprisingly large magnetic moments, especially on the comparatively exposed O1 site. Thus, it appears that the electron holes required to neutralize the surface are located largely on the oxygen atoms in the second layer, opening up the formally closed shell of the oxide anion and revealing magnetic moments in the process. (Since our model employs very compact basis sets, we wish to stress here that the magnitude of the magnetic moment – especially the large O moments – should not be taken as an absolute value,

but rather as evidence for some magnetic polarization). O1 is located on top of a triangle of Ni2 sites, and comparison of the LDOS of O1 and Ni2, clearly evinces bands around the Fermi level common to both sites. The Ni atom in the top layer (Ni1) – sited exposed on top of a triangle of oxygen atoms (O2 sites) – also exhibits a fair reduction of its partial charge. However, we suggest that this is largely due to an increased covalency since this atom, in comparison with bulk, has lost three of its six nearest oxygen neighbors. Through increased covalency, Ni1 effectively gains electrons, largely at the expense of the O2 site – this is evident in the fact that the partial charge on O2 is somewhat smaller than that of the O1 site in the same layer (-0.83 vs. -1.19 e). The much smaller fluctuations in charge and moments of atoms in the third (Ni2), fourth (O3, O4) and fifth layer (Ni3, Ni4) are probably due to small changes in covalency that are induced by the nearby vacancies, slightly changed local interatomic distances to nearest neighbors, as well as the stray fields due to the charge turmoil in the layers above. Ni2 has a complete set of six nearest oxygen neighbors – thus, its partial charge is only slightly reduced with respect to bulk (+1.59 vs. +1.73 e) and its LDOS structure is already fairly close to that of Ni in bulk NiO.

Similar DFT electronic structure calculations as well as atomistic simulations were performed on the Ni- and O-terminated octopolar reconstructions proposed by Barbier et al. [13,14].

The atomistic model yielded surface energies of 2.70 and 2.71 J/m² for the Ni- and O-terminated octopolar reconstructions, respectively, far too close to make a clear call between the two alternatives. Since the two reconstructions differ only by the interchange of all Ni atoms for O atoms and vice versa, this result is not much of a surprise, considering that the interactions between atoms in the model potential are almost symmetric with respect to interchange of atom types, especially in the dominant electrostatic terms. The only asymmetry in the model is in the polarizability term for oxygen atoms and the O–O Buckingham potential. The atomistic model is of course a representation of the real situation near the surface; thus, the observation of very close surface energies for

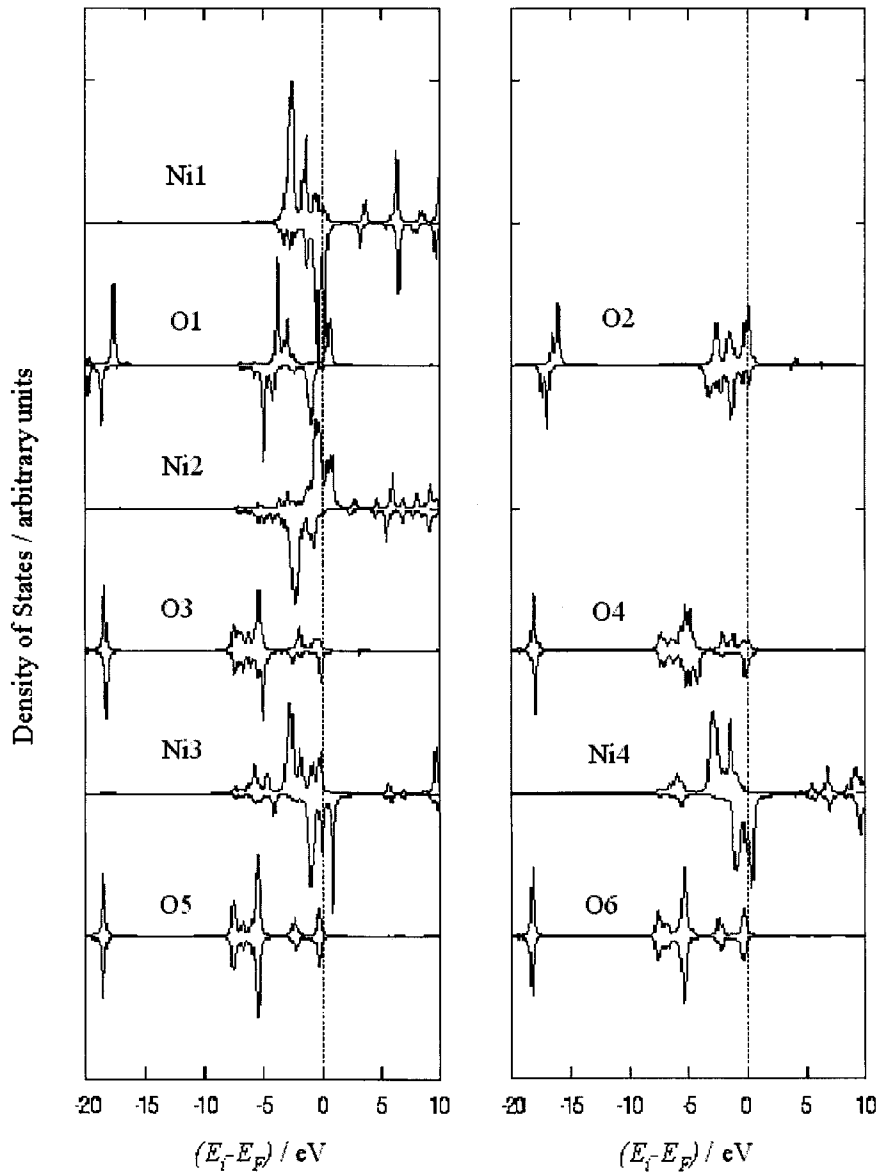


Fig. 6. Depth profile of LDOS calculated for the oxidized surface reconstruction proposed in this work. LDOS plots of symmetry non-equivalent atom types located in the same atomic layer are plotted next to each other.

Ni- and O-termination gives support to the stipulation of coexisting Ni- and O-terminated phases [13,14], if indeed NiO(111) forms stoichiometric octopolar reconstructions.

Another effect of the near atom-interchange symmetry of the interaction potential was that calculated geometries for Ni- and O-terminated

octopolar reconstructions are very similar indeed. For the purposes of the following discussion, we have listed in Table 3 the relaxed atomic positions for the Ni-terminated reconstruction only and omitted for brevity those for the O-terminated reconstruction. A side view of the surface is given in Fig. 7. Particularly noteworthy in this recon-

Table 3

Atomistically relaxed atom positions and relevant inter-atomic distances calculated for the Ni-terminated octopole structure in terms of $p(2 \times 2)$ unit cell in $p3m1$ plane group with $a = b = 5.8970 \text{ \AA}$, $c = 40.0 \text{ \AA}$, $\alpha = \beta = 90^\circ$, $\gamma = 120^\circ$

Layer	Atom	x/frac	y/frac	$z/\text{\AA}$
1	Ni1 (1 \times)	0	0	0.000
2	O2 (3 \times)	0.306	0.153	0.829
3	Ni3 (1 \times)	2/3	1/3	1.194
	Ni4 (3 \times)	0.160	0.320	2.050
4	O3 (1 \times)	0	0	3.166
	O4 (3 \times)	1.023	0.511	3.033
5	Ni5 (1 \times)	1/3	2/3	4.269
	Ni6 (3 \times)	0.829	0.658	4.214

Ni1–O2: 1.771 \AA , Ni3–O2: 1.876 \AA , Ni4–O2: 2.013 \AA , Ni3–O4: 2.587 \AA , Ni4–O3: 1.979 \AA , Ni4–O4: 1.951 \AA .

struction is the considerably reduced bond length of 1.9 \AA between Ni3 and O2, as well as the much expanded bond length between Ni3 and O4 of 2.6 \AA . Closer inspection of the structure reveals that the third layer of Ni3 and Ni4 atoms exhibits quite a considerable splitting in vertical direction (z) with Ni3 almost merging into the second layer (O2 atoms). We find a vertical separation of 0.88 \AA between Ni3 and Ni4 layers, whereas the vertical separation between the Ni3 and O2 is only 0.36 \AA . These rather large changes in the atomic positions

away from those reported by Barbier et al. [13,14] support the conclusion based upon fitting the intensity data (described above) that simple Ni- or O-terminated octopoles are not the correct structure for this surface.

Calculated partial atomic charges and magnetic moments for the first few atomic layers of Ni- and O-terminated octopolar reconstructions are listed in Table 4. In comparison to what was found for our oxidized reconstruction (Table 2), the calculated atomic charges for the octopolar surfaces exhibit a considerably smaller surface effect. No electron holes are required for charge neutrality of these surfaces and the only surface effects are due to changes in degree of covalence and charge transfer between atoms due to reduced coordination or changes in bond lengths. The largest charge differences are found for the atoms in the top layer, Ni1 and O1 for Ni- and O-terminated reconstructions, which carry partial charges of +1.49 and -1.53 , respectively, vs. ± 1.71 for bulk.

4. Discussion

The reconstruction is very simple and can be characterized by alternating close-packed layers of

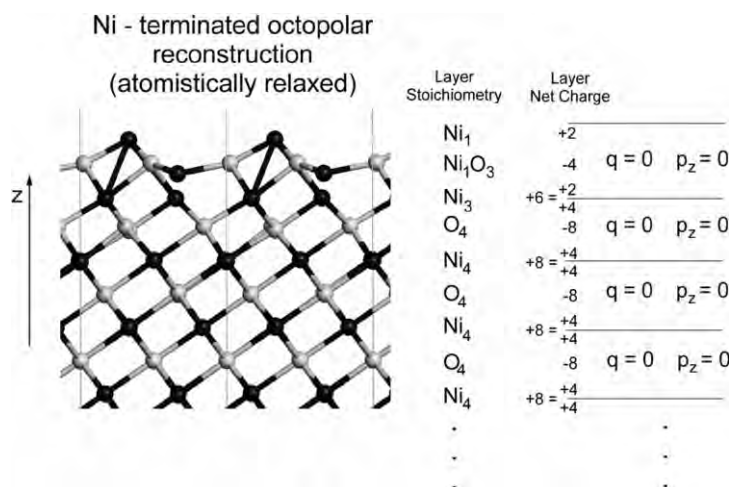


Fig. 7. Side view of the atomistically relaxed, Ni-terminated octopolar reconstruction of NiO(111). On the side, stoichiometries and net-charges of stacked layers are listed. For the purpose of charge accounting, O and Ni atoms with small vertical separations were merged together into a single layer of stoichiometry Ni₁O₃ (cf. text). The right-hand side of the figure illustrates that layer charges are arranged such that slabs of zero charge (q) and vertical dipole moment (p_z) result.

Table 4

Atomic partial charges and magnetic moments (in brackets) calculated for the top five layers of atomistically relaxed Ni- and O-terminated octopole reconstructions

Layer	Ni-terminated octopolar reconstruction		O-terminated octopolar reconstruction	
	Element	Charge/e (moment/ μ_B)	Element	Charge/e (moment/ μ_B)
1	Ni1 (1 \times)	+1.49 (+0.89)	O1 (1 \times)	-1.53 (+0.33)
2	O2 (3 \times)	-1.60 (-0.11)	Ni2 (3 \times)	+1.60 (+1.20)
3	Ni3 (1 \times)	+1.82 (-1.33)	O3 (1 \times)	-1.67 (+0.18)
	Ni4 (3 \times)	+1.59 (-1.32)	O4 (3 \times)	-1.65 (-0.08)
4	O3 (1 \times)	-1.72 (-0.19)	Ni3 (1 \times)	+1.73 (-1.67)
	O4 (3 \times)	-1.67 (-0.04)	Ni4 (3 \times)	+1.69 (-1.36)
5	Ni5 (1 \times)	+1.74 (+1.70)	O5 (1 \times)	-1.71 (+0.12)
	Ni6 (3 \times)	+1.74 (+1.65)	O6 (1 \times)	-1.71 (+0.11)

oxygen and nickel atoms. The top surface layer is nickel-terminated, with 3/4 of the nickel atoms missing, the next oxygen layer is completely full, and the third (nickel) layer has 1/4 of its nickel atoms missing. The structure can also be described in terms of defect chemistry: consider an oxygen-terminated bulk NiO(111), then introduce a Schottky type defect into the lattice using 1/4 of the available Ni²⁺ sites in the next close-packed layer; i.e., create a vacancy by removing one positive ion (Ni²⁺) and placing it on the surface.

The structure exhibits the features observed by the STM study [12] – several missing-atom point defects and a nanofacet structure (with in effect three {100} type facets) created by the octopolar units on the surface (Fig. 8). The STM images showing atomic trimers in a (2 \times 2) arrangement were taken at a negative sample bias [12]; i.e., electrons tunneling from the sample to the STM tip, thus imaging – as conventional wisdom holds –

the valence- (oxygen-) band. This is in agreement with the structure, with an oxygen trimer underneath a single nickel atom. At lower negative bias only a single atom is visible which corresponds to the exposed single Ni atom in the top layer of the surface.

The surface structure reported in this work differs in some aspects from other (2 \times 2) reconstructions reported in the literature for NaCl-type polar oxide surfaces, specifically from the atomically faceted octopole surface structures [8,9]. In particular, our reconstruction is clearly different from the coexisting Ni- and O-terminated octopolar reconstructions proposed by Barbier et al. [13,14] through Patterson analysis of the thin film GIXS data. Near identical surface energies and atomic positions from the atomistic model for Ni- and O-terminated octopolar reconstructions are in support of the coexisting octopolar surface model; however, it appears to be contradicted by the STM

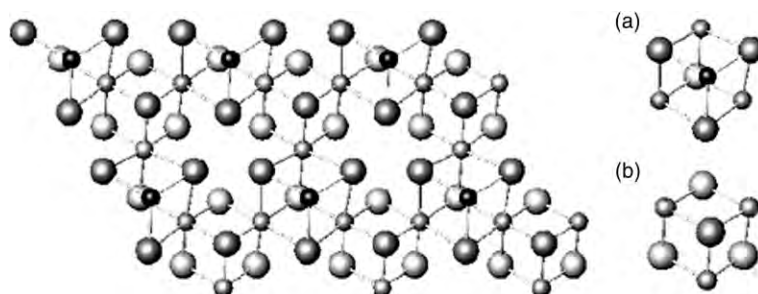


Fig. 8. Top view of the oxidized $p(2 \times 2)$ NiO(111) reconstruction with only top three (surface) layers shown (the structure is rotated 6 deg. about z -axis from configuration shown in Fig. 4). The surface can be constructed using (a) nickel-terminated and (b) oxygen-terminated octopolar blocks.

observation of a single-phase material [12]. We also wish to point out, that the strong vertical displacement of the Ni3 layer away from Ni4 towards the O2 layer (for Ni-termination, and similar for O-termination), is not observed in the experimental relaxations found by Barbier et al. [14] (vertical splitting Ni3/Ni4: $\delta_{2S} - \delta_2 = 0.078$ Å in Ref. [5] vs. 0.88 Å in this work). As will be argued below, we consider the merging of Ni3 and O2 layers an important aspect of structural stability.

Clearly, the driving principle of surface reconstruction is that the surface seeks to minimize its internal energy, which in an ionic material is largely electrostatic in nature. The octopole model is largely based on the argument that a simple cubic, or ‘octopolar’, arrangement of eight atoms (four atoms each of opposite charge) has a rapidly decaying interaction potential with other octopoles [9]. The {100} faceted octopole reconstructions proposed in the literature [9,13,14] for the NiO(111) surface are based on that model. Since construction of the polar surfaces solely from octopolar (NiO)₄ building blocks is limited to stoichiometric surfaces, non-stoichiometric reconstructions such as ours do not readily fit into this model. A stability argument for the present oxidized (cation deficient) surface has to address the fact that it is constructed not only from (NiO)₄ building blocks but also some “left-over” atoms. In addition, oxidation of this surface is characterized by the presence of electronic defects (e⁻ holes) near the surface. The precise location of these (positively charged) electron holes is clearly very relevant to any discussion of electrostatic stability.

Interesting in this context is that the atomistically relaxed octopolar reconstruction has the Ni3 site vertically relaxed towards the second O2 layer. This being the case, one may consider Ni4 forming its own separate layer, while Ni3 almost merges into the O2 layer; i.e., the stacking is more adequately described as bulk-Ni₄-O₄-Ni₃-(Ni₁O₃)-Ni₁ as opposed to bulk-Ni₄-O₄-Ni₄-O₃-Ni₁. The merit of such a reformulation is that now the electrostatics of the Ni-terminated octopolar reconstruction can be directly compared to that of our oxidized reconstruction, which is characterized by the stacking sequence ...-O₄-Ni₄-O₄-Ni₃-(O₄+4h)-Ni₁. In this, 4h denotes the pres-

ence of the four electron holes required for charge neutrality, which were found to be located in the second layer (see above). A comparison of electrostatic stability is possible because the stacking of these two reconstructions differs only in the second layer, where a (Ni₁O₃) stoichiometry is replaced by (O₄+4h), both having the same formal net-charge of -4. As is illustrated in Fig. 7, this kind of stacking of charged layers, although idealized, suggests a high degree of stability since all dipole components perpendicular to the surface vanish. Clearly, this electrostatic model is very simplified and idealized; however, we believe it provides a simple explanation for (a) the displacement of Ni3 atoms towards the O2 layer in the Ni-terminated octopolar reconstruction, (b) electron holes being located in the second (oxygen) atom layer of the oxidized construction, and thus (c) suggests that our oxidized and the stoichiometric octopolar reconstructions may be comparable in terms of electrostatic stability.

In conclusion, we find the termination of thin film NiO(111) by direct methods analysis of GIXS diffraction data, to be single-phase, Ni-terminated, and cation deficient with 3/4 of top layer and 1/4 of third layer atoms vacant. Our reconstruction differs from the previously proposed bi-phasic octopolar reconstruction model [13,14], but is in better agreement with the STM study of Ventrice et al. [12].

Acknowledgements

We would like to acknowledge Dr. A. Barbier for supplying us with the GIXD data set for this work. This work was supported by the EMSI program of the National Science Foundation and the US Department of Energy Office of Science (CHE-9810378) at the Northwestern University Institute for Environmental Catalysis. This work was also supported in part by the Department of Energy (under grant no. DE FG02 84ER45097).

References

- [1] H.J. Freund, Phys. Stat. Sol. B 192 (1995) 407.
- [2] M.A. Banares, Cat. Today 51 (1999) 319.

- [3] A.Z. Men'shikov, Y.A. Dorofeev, A.E. Teplykh, B.A. Gizhevskiy, N.A. Mironova, *Phys. Sol. State* 42 (2000) 315.
- [4] S.G. Christoskova, N. Danova, M. Georgieva, O.K. Argirov, D. Mehandzhiev, *Appl. Cat. A* 128 (1995) 219.
- [5] C. Mitsui, H. Nishiguchi, K. Fukamachi, T. Ishihara, Y. Takita, *Chem. Lett.* 12 (1999) 1327.
- [6] F. Bertaut, *Comput. Rendu.* 246 (1958) 3447.
- [7] A. Gibson, R. Haydock, J.P. LaFemina, *J. Vac. Sci. Technol. A* 10 (1992) 2361.
- [8] A.C. Shi, M. Wortis, *Phys. Rev. B* 37 (1988) 7793.
- [9] D. Wolf, *Phys. Rev. Lett.* 68 (1992) 3315.
- [10] P.M. Oliver, G.W. Watson, S.C. Parker, *Mod. Simul. Mater. Sci. Engng.* 1 (1993) 755.
- [11] M.A. Schofield, R.A. Plass, D. Grozea, L.D. Marks, M. Gajdardziska-Josifovska, *Surf. Sci.*, submitted for publication.
- [12] C.A. Ventrice Jr., Th. Bertrams, H. Hannemann, A. Brodde, H. Neddermeyer, *Phys. Rev. B* 49 (1994) 5773.
- [13] A. Barbier, G. Renaud, C. Mocuta, A. Stierle, *Surf. Sci.* 433–435 (1999) 761.
- [14] A. Barbier, C. Mocuta, H. Kuhlenbeck, K.F. Peters, B. Richter, G. Renaud, *Phys. Rev. Lett.* 84 (2000) 2897.
- [15] L.H. Schwartz, J.B. Cohen, *Diffraction from Materials*, second ed., Springer, Berlin, 1987, pp. 303–312.
- [16] L.D. Marks, D. Grozea, R. Feidenhans'l, M. Nielsen, R.L. Johnson, *Surf. Rev. Lett.* 5 (1998) 459.
- [17] C. Collazo-Davila, D. Grozea, L.D. Marks, R. Feidenhans'l, M. Nielsen, L. Seehofer, L. Lottermoser, G. Falkenberg, R.L. Johnson, M. Gothelid, U. Karlsson, *Surf. Sci.* 418 (1998) 395.
- [18] L.D. Marks, *Phys. Rev. B* 60 (1999) 2771.
- [19] L.D. Marks, E. Bengu, C. Collazo-Davila, D. Grozea, E. Landree, C. Leslie, W. Sinkler, *Surf. Rev. Lett.* 5 (1998) 1087.
- [20] L.D. Marks, W. Sinkler, E. Landree, *Acta Cryst.* 55 (1999) 601.
- [21] G.M. Sheldrick, SHELX-97, University of Göttingen.
- [22] H.X. Gao, L.M. Peng, J.M. Zuo, *Acta Cryst. A* 55 (1999) 1.
- [23] <http://www.numis.nwu.edu/SurfaceDiffraction/xray.html>.
- [24] D.E. Ellis, G.S. Painter, *Phys. Rev. B* 2 (1970) 2887.
- [25] E.J. Baerends, D.E. Ellis, P. Ros, *J. Chem. Phys.* 2 (1973) 41.
- [26] A. Rosen, D.E. Ellis, H. Adachi, F.W. Averill, *J. Chem. Phys.* 65 (1976) 3629.
- [27] W. Yang, *Phys. Rev.* 66 (1991) 1438.
- [28] W. Yang, T.S. Lee, *J. Chem. Phys.* 103 (1995) 5674.
- [29] O. Warschkow, J.M. Dyke, D.E. Ellis, *J. Comp. Phys.* 143 (1998) 70.
- [30] O. Warschkow, Ph. D. Thesis, University of Southampton, 1999.
- [31] K. Terakura, T. Oguchi, A.R. Williams, J. Kübler, *Phys. Rev. B* 30 (1984) 4734.
- [32] A. Svane, O. Gunnarson, *Phys. Rev. Lett.* 9 (1990) 1148.
- [33] J. Zaanen, G.A. Sawatzky, J.W. Allen, *Phys. Rev. Lett.* 55 (1984) 418.
- [34] M.D. Towler, N.L. Allen, N.M. Harrison, V.R. Saunders, W.C. Mackrodt, E. Apra, *Phys. Rev. B* 50 (1994) 5041.
- [35] P. Wei, Z.Q. Qi, *Phys. Rev. B* 49 (1994) 10864.
- [36] M. Yan, S.P. Chen, T.E. Mitchell, D.H. Gay, S. Vyas, R.W. Grimes, *Phil. Mag. A* 72 (1995) 121–138.
- [37] J.D. Gale, GULP (General Utility Lattice Program), Royal Institution, London.
- [38] J.D. Gale, *Phil. Mag. B* 73 (1996) 3.